Nanocrystalline Silicon Superlattices for Nanoelectronic Devices

Leonid Tsybeskov

Department of Electrical and Computer Engineering,
New Jersey Institute of Technology, Newark, NJ
tsybesko@adm.njit.edu

ABSTRACT

This paper provides a brief introduction to a novel nanostructured system consisting of ordered layers of Si nanocrystals separated by atomically flat and chemically abrupt layers of amorphous silicon dioxide with thickness of several nanometers. The unique structural, optical and electrical properties permitting unusual device application are discussed.

1. INTRODUCTION

The quest for functional Si/SiO_2 quantum structure has a long history originating with the pioneering tunnel diode work of Esaki and Miyahara in 1960. Since that time, the demand for a Si based quantum structure with well-defined potential barriers and defect-free interfaces remains unsatisfied, as Si/Ge heteroepitaxy has never reached the level of III-V materials. Recent success in fabricating robust nanocrystalline Si / SiO_2 superlattices (SL) using controlled crystallization of nanometer thin a-Si layers confined between SiO_2 layers [1-4] depicts another avenue for a Si based quantum structure. In this structure, the Si layer is not a single crystal but consists of similarly shaped, nearly equal in size Si nanocrystals with additional possibility to control their crystallographic orientation [4]. Atomically flat and chemically abrupt SiO_2 layers separate the Si nanocrystals and provide deep carrier confinement [5, 6], which is a key condition for functional quantum devices. This paper summarizes recent results on nanocrystalline silicon (nc-Si)/ amorphous silicon dioxide (a-SiO_2) SL fabrication, characterization and exploratory applications in novel device structures.

2. SAMPLE FABRICATION AND STRUCTURAL CHARACTERIZATION

The details of sample preparation are described in a number of papers [1-4] and summarized in this work. The majority of studied samples are prepared using magnetron sputtering of the a-Si and amorphous SiO_2 multilayers in a Perkin-Elmer 2400 sputtering system by radio-frequency (RF) sputtering and plasma oxidation. A substrate usually is a single crystal Si wafer covered by thermally grown SiO_2 layer, and substrate temperature during the sputtering is varied from room temperature to 400^{o}C. The sputtering rate can be controllably changed from 3Å to 25 Å per minute, and that allows reproducible deposition of a-Si layers with thickness in the range from 20Å to 250 Å. The thickness of a-SiO_2 is usually kept between 15Å and 60 Å. Depending of particular measurements, the number of periods is varied from 1 to 60. After the deposition of an a-Si/a-SiO_2 SL, thermal crystallization of the structure is performed in two steps: (1) rapid (40-60 s) thermal annealing (RTA) at 800-900^{o}C followed by (2) furnace annealing up to 1100^{o}C for an hour. The role of the double-step annealing is to create crystalline nuclei by RTA (nucleation stage) and to complete the crystallization of the Si nanocrystals and improve their surface passivation (growth stage). After nucleation, the nanocrystalline nuclei are surrounded by an amorphous tissue and occupy not more than ~ 20-30% by volume of the Si layer (estimated from Raman scattering). After furnace annealing nearly 90-95% of the Si volume is crystallized if Si nanocrystals are greater than 30 Å in diameter.

As we have shown [1-3], the thermal crystallization of a-Si/SiO_2 multilayers is controlled by several factors. Silicon has a very low diffusivity in SiO_2 and the initial RTA process forms nanocrystals without distorting the SL periodic structure. In addition, after the formation of Si nuclei, the crystallization is favorable thermodynamically due to strongly covalent nature of Si-Si bonds. Vertically, silicon crystallization proceeds until it reaches the Si-SiO_2 interface where it stops due to the amorphous nature of silicone dioxide. Laterally, silicon crystallization is limited only by the nanocrystal interaction with each other. In other words, Si nanocrystal grain boundaries prevent formation of a continuous single crystal Si layer. We found that the shape of the Si nanoclusters with diameter of $\leq$ 50-60Å is almost spherical, and that is due to a competition between surface and volume tension. For nanocrystals with

vertical dimension of > 200 Å, a distinct brick-like shape with an extended lateral size up to 500 Å is observed [4]. The specific mechanism, which could be responsible for brick-like nanocrystal shape is discussed in Ref. . Another important issue in layered Si/SiO_2 structure is the presence of strain, and that is due to difference in bond arrangement (length and angles) and thermal expansion in Si and SiO_2. The strain reduction in nc-Si/SiO_2 multilayers is achieved due to discontinuity of the Si layer. The studied structures exhibit a moderate ($< 10^{11}$ cm^{-2}) density of the Si/SiO_2 interface defects [5].

A wide variety of structural characterization techniques have been applied to study the nc-Si SLs. X-ray specular reflectivity measurements were carried out using a Philips PW1820 vertical goniometer and simulated using the Philips HRS calculation package. The Raman experiments were carried out at room temperature in a quasi-backscattering geometry using a Jobin-Yvon triple spectrometer or a Spex 14018 double spectrometer. Low-frequency Raman scattering was also measured using a SOPRA DMDP 2000 double monochromator with a cooled Hamamatsu R928P photomultiplier. The excitation source was 300 mW of 457.9 nm Ar^+ laser light with an angle of incidence of 77.7^o.

Auger elemental microanalysis was performed with a Physical Electronics Industries PHI 650 instrument with a 5 keV electron beam 30^o off normal. The TEM analysis was performed with a Philips EM 430 microscope operated at 300 kV. Electrical measurements were performed at temperatures ranging from 20 to 300 K in a closed-cycle CTI-Cryogenic system using a Keithly 220 current source and a Keithly 595 quasi-static CV meter.

2.1 Transmission Electron Microscopy

Figure 1 compares TEM micrographs of nc-Si SLs with 42 Å (Fig. 1a) and 85 Å (Fig. 1b) and Figure 2 shows a sample with 200 Å thick nc-Si layers crystallized under the same conditions. We found that a 42 Å-thick nc-Si layer consists mostly of spherical and elliptical nanocrystals with significant variations in their shape. An 85 Å-thick nc-Si layer consists mainly of square-shaped Si nanocrystals. For both samples the SiO_2 separating layers look planar. A SL with a 200 Å thick nc-Si layer contains well-defined, brick-shaped Si nanocrystals with a lateral dimension 2.2 - 2.5 times larger than the vertical dimension. Figure 2b shows a detailed image of a perfectly shaped Si nanocrystal brick with a lateral size of ~ 500 Å and a vertical size of 200 Å. The propensity to form bricks of nc-Si is just one remarkable feature of this novel system. As it has been shown [4], brick-shaped nanocrystals exhibit preferred crystallographic orientation and better interfaces with more abrupt chemical composition and a lower interface defect density.

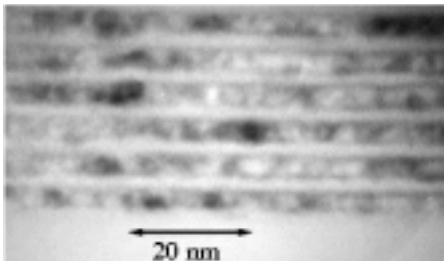

(a)

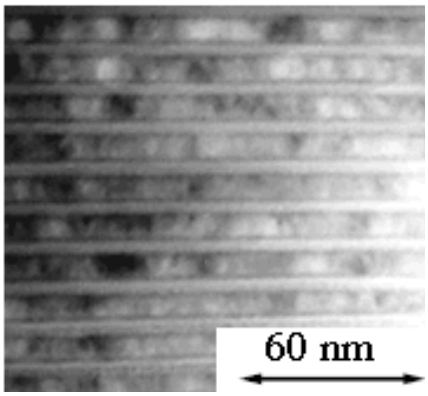

(b)

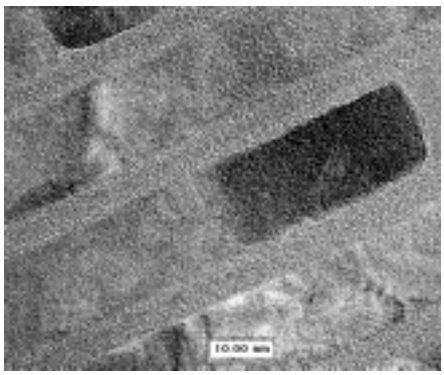

(c)

Figure 2. TEM micrograph of (a) nearly spherical Si nanocrystal with 45A diameter nanocrystals, (b) laterally extended nanocrystals with 85A vertical dimension, and (c) brick-shaped nanocrystals with 200A vertical and 500A lateral dimensions showing nearly atomically flat interfaces [4].

3. EXPERIMENTAL

3.1 Low-frequency Raman scattering: acoustic phonons folding

The TEM analysis in samples containing Si nanocrystals is complicated by the absence of single crystal planes over the entire sample area. Therefore, such an analysis needs to be complemented by another characterization technique such as inelastic light scattering. The

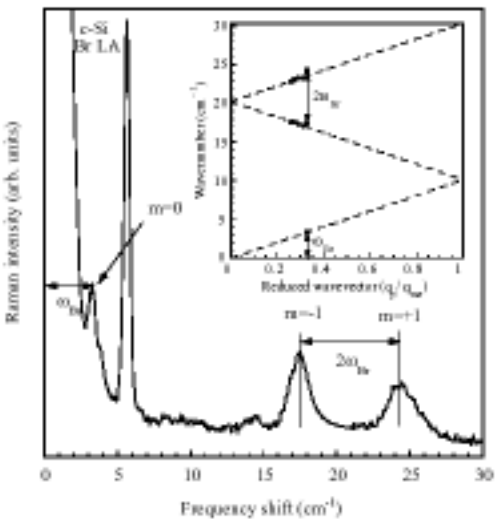

Figure 2. A high resolution (< 0.06 cm^{-1}) spectrum of inelastically scattered light in a 20 period 85Å nc-Si/35Å nm a-SiO_2 SL, shows Brillouin scattering from the SL and crystalline Si substrate, and Raman scattering from the first pair of FLA phonons. The partial reconstruction of the Brillouin minizone using excitation at different wavelengths is shown in the inset [4].

Raman spectrum from an 85 Å nc-Si / 35 Å a-SiO_2 SL with 20 periods is shown in Figure 2. A high spectral resolution and very low diffusive scattering permit the observation and identification of scattering from the zero-order (or Brillouin scattering) peak at ω_{Br}=3.4 cm^{-1} and the first doublet of SL folded longitudinal acoustic (FLA) phonons m=±1 at ω_{-1}=17.4 cm^{-1} and ω_{+1}=24.3 cm^{-1}. Note, that $\omega_{+1}-\omega_{-1}=2\omega_{Br}$, exactly as expected from the theory. The Brillouin minizone for this sample was reconstructed using the measured $\omega_{\pm\mu}$ and the calculated normalized phonon wavevectors $q_p(\lambda)/q_{mz}=2(\omega_{+1}-\omega_{-1})/(\omega_{+1}+\omega_{-1})$. The use of different wavelengths in the excitation allowed the observation of inelastic light scattering from the LA phonons with normalized wavevectors in the 0.26-0.31 range, where the phonon dispersion is expected to be linear. By fitting the experimental data, we calculated the overall nc-Si / SiO_2 SL sound velocity as v_{SL}= (7.5±0.2)·10^5 cm/s, and the sound velocity in 85Å Si nanocrystals as $v_{nc\text{-}Si}$=(8.7±0.5)·10^5 cm/s. The latter number is close to the sound velocity in c-Si along the <100> direction ($v_{Si<100>}$=8.5·10^5 cm/s), and this result suggests that Si nanocrystals within nc-Si SLs are not oriented randomly.

Raman scattering associated with FLA phonon modes have been studied in nc-Si SLs with different thicknesses of nc-Si layers. The result indicates a qualitative difference in the scattering from FLA modes for samples with different Si nanocrystal sizes. This difference may be associated with (1) an increase of the nc-Si/SiO_2 interface roughness, and/or (2) changes in the average Si nanocrystals crystallographic orientation. For randomly oriented Si nanocrystals the averaging of sound velocities along different Si crystallographic directions (varying from 8.5 10^5 cm/s to 9.2 10^5 cm/s) should broaden the FLA signal and decrease the peak-to-valley ratio. This result also indicates that Si nanocrystals with a vertical size larger than 80Å may have a preferred crystallographic orientation. Performing polarized Raman scattering measurements, we have proved the existence of preferential crystallographic orientation in nc-Si SLs [4].

3.3 Tunnel spectroscopy in nc-Si superlattices: a tunnel diode prototype

Current tunnel spectroscopy (CTS) is one of the most sensitive techniques available to characterize junctions and interfaces. In order to apply CTS, we fabricated a double-barrier structure with a single ~ 130Å-thick nc-Si layer sandwiched between two tunnel-transparent a-SiO_2 layers of thickness ~ 15Å. The structure was deposited on a heavily doped p+ Si substrate (resistivity of ~ 0.01 Ω cm) with an Al / n+ doped polycrystalline Si top contact (Fig. 4, inset). The structure is similar to the Esaki diode, because the electron injected from the top contact should tunnel across the 130Å layer of Si to the heavily B-doped substrate. The experiment was performed at 15 K to minimize thermal broadening and the electron-phonon interaction. In order to clarify the details, we have used the second derivative of the I-V data. Several features corresponding to different phonon and phonon-combination energies (TO, TA, etc.) are observed (Fig. 3). The observation of phonon-assisted transitions in the interband tunneling

indicates a feasibility of nc-Si/a-SiO_2 device applications.

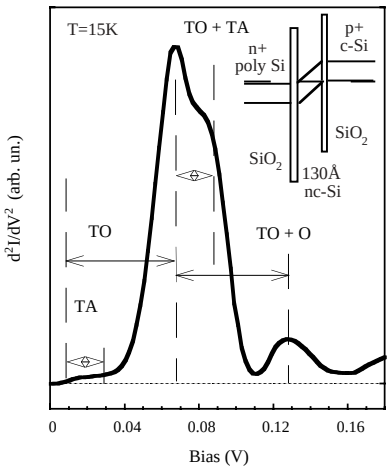

Figure 4. Second derivative of the I-V curve in a structure consisting of Al/3000Å n+ polycrystalline Si contact / 15Å a-SiO_2 / 130Å nc-Si / 15Å a-SiO_2 / p+ c-Si substrate. Different phonon energies are shown. The tunnel current threshold of the ~ 46 mV indicates a small, built-in potential, possibly due to a localized charge [5].

3.4 Can resonant tunneling be achieved in partially disordered nanostructures?

In a wide variety of phenomena associated with carrier quantum transport, resonant carrier tunneling (RCT) and negative differential conductivity (NDC) due to a non-monotonic dependence of the electron tunnel transmission through potential barriers has always been associated with nearly perfect semiconductor heterostructures with a long carrier mean free path. At the same time, the question as to how RCT can be preserved in a structure exhibiting partial disorder remains important both for academic interest in quantum structures and for practical quantum device applications. Thus, a system with a controlled degree of disorder, combining for example a periodic potential in the Z direction (*i.e.*, the growth direction) with the presence of grain boundaries separating nanocrystals laterally in the XY plane, would form a special case of general interest. A nc-Si SL fabricated by controlled crystallization of amorphous Si/SiO_2 layered structures is a perfect example of such a system. Our results [7] show that in such nc-Si/SiO_2 system with large potential barriers, resonant tunneling and the formation of electron standing waves surprisingly remains possible despite significant carrier scattering.

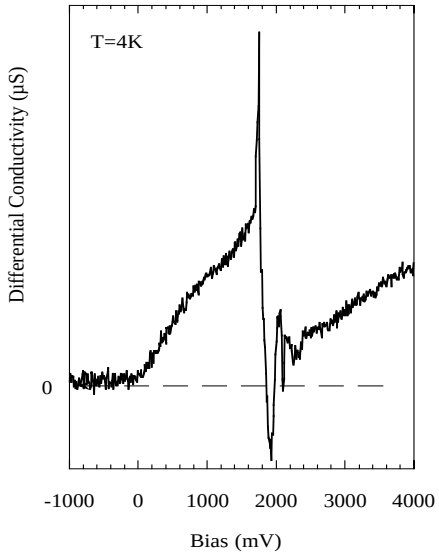

Figure 5. Experimental observation of low temperature NDC in nc-Si /SiO_2 SLs. Vertical excess is differential conductivity (a.u.), horizontal is voltage (200 mV/div.)

4. CONCLUSION

Using a technique of thermal crystallization we have produced nc-Si SLs with angstrom-level flat and chemically abrupt nc-Si/a-SiO_2 interfaces. The interface defect density is found to be in the order of tolerance for a standard CMOS device [5]. We have showed that resonant tunneling and NDC can be achieved in a structure containing considerable imperfections such as grain boundaries between Si nanocrystals [7].

REFERENCES

1. L. Tsybeskov et. al., Appl. Phys. Lett. **72**, 43 (1998).
2. L. Tsybeskov et. al., Physica Status Solidi **165**, 69 (1998).
3. L. Tsybeskov et. al., MRS Bulletin **23** (4), 1998.
4. G. F. Grom et. al., **Nature 407**, 358 (2000).
5. L. Tsybeskov et.al., Appl. Phys. Lett., **75**, 2265 (1999).
6. L. Tsybeskov et. al., Materials Science and Engineering **B 69-70**, 303-308 (2000)
7. L. Tsybeskov et al., Euro Physics Letters, **55** (4), 552 (2001).